Three-dimensional Finite-element Analysis of Joule Heating in Electrochemotherapy and *in vivo* Gene Electrotransfer

Igor Lacković, Ratko Magjarević
University of Zagreb
Faculty of Electrical Engineering and Computing
10000 Zagreb, Croatia

and **Damijan Miklavčič**
University of Ljubljana
Faculty of Electrical Engineering
1000 Ljubljana, Slovenia

ABSTRACT

Electrochemotherapy and electrogene therapy are new methods in molecular medicine based on electroporation-mediated introduction of foreign molecules (chemotherapeutic drugs, DNA) into target cells *in vivo*. Electrochemotherapy involves the injection of chemotherapeutic agent followed by a local delivery of a train of short high-voltage pulses to the tumor nodule (i.e. 8 square-wave pulses of 100 μs duration delivered at the repetition frequency of 1 Hz or several kHz, with a voltage-to-distance ratio of up to 1500 V/cm). For the transfer of DNA across a cell membrane a train of long low-voltage pulses (i.e. 8 rectangular pulses of 50 ms duration delivered at the repetition rate of 1 Hz, with a voltage-to-distance ratio up to 250 V/cm) is much more effective due to the electrophoretic effect on DNA molecule. In this paper we present a comprehensive analysis of tissue heating as a potential side effect of electric pulses used for electroporation-based treatments. The analysis is based on a coupled electro-thermal model using 3-D finite-element approach. We studied two electrode geometries: parallel plates and a pair of needles. By setting the appropriate boundary conditions, we simulated driving of electrodes with short, high-voltage, electropermeabilizing pulses and with longer, lower voltage, electrophoretic pulses. We obtained time dependent solutions for electric field and temperature distribution by FEM solver. Based on the numerical simulations we analyzed the influence of tissue electrical conductivity and parameters of electric pulses (amplitude, duration, number of pulses, pulse repetition frequency) on the temperature distribution within the tissue and the electrodes. Results of our simulations show that at specific pulse parameters at least locally tissue heating might be significant (i.e. tissue temperatures to grow in excess of 43ºC). For electrochemotherapy, this is not critical, but DNA electrotransfer may be unsuccessful due to heating-related DNA damage or denaturation.

Index Terms — Electroporation, electrochemotherapy, electrogenetherapy, tissue field strength, Joule heating, finite element method.

1 INTRODUCTION

ELECTROCHEMOTHERAPY is a term used to describe the enhancement of antitumor effectiveness of chemotherapeutic drug by the local application of electric pulses of appropriate characteristics at the tumor site. The method was tested on animal tumor models [1-6], first reports and clinical trials in humans were encouraging [7-13], and electrochemotherapy is now clinically acknowledged method for the treatment of cutaneous and subcutaneous tumors [14]. The prerequisite for the antitumor effect, in addition to the proper choice of cytotoxic agent, is the application of sufficiently large electric field to tissue. The underlying physical and chemical processes associated with the effect of large electric fields to cells in tissue are still not fully explained. However, the results of experimental studies and predictions of theoretical models indicate that cell membrane, when exposed to high enough electric field, goes through a process of structural rearrangements and becomes permeable to ions and various molecules (drugs, proteins, DNA, etc.) that otherwise have hampered transport through the cell membrane. This phenomenon is termed membrane electroporation where electropermeabilization is used to describe its most important

outcome – increased permeability of cell membrane [15-19]. Namely, it is believed that the enhanced uptake of exogenous molecules into the cells is due to formation of transient aqueous pores in the lipid bilayers. If the electric field is not too high, membrane reseals and cell viability is preserved. Besides electrochemotherapy, the application of intense electric pulses for *in vivo* transfer of DNA into living cells, known as *in vivo* gene electrotransfection, is rapidly expanding [20-26]. This is safer alternative for DNA transfer than using viral vectors. Studies of plasmid DNA transfer into skeletal muscle have shown that efficient long-term expression can be achieved [22]. Electroporation-based methods of gene delivery are also feasible in transfecting solid tumors [23, 25]. Therefore we can expect that *in vivo* gene electrotransfer will also become safe and efficient method for gene therapy.

For successful electrochemotherapy and *in vivo* gene electrotransfection it is important to reversibly permeabilize cells in the target area and at the same time to minimize the area where cell necrosis occurs. The governing factor for cell permeabilization is the intensity of the local electric field in tissue which is the result of applied voltage, electrode geometry and tissue properties. Numerous experimental studies dealt with the optimization of pulse amplitudes, pulse width and the number of pulses for electrochemotherapy of tumors and for *in vivo* gene electrotransfer. For internalization of smaller molecules into the cells, short, high intensity pulses are used. However, for transfer of macromolecules, such as DNA, much longer pulses are preferred since electrophoretic effect of electric pulses on DNA molecules is important for its transfer across the cell membrane. In electrochemotherapy of tumors, the most widely used protocol comprises of eight pulses having duration of 100 μs, repetition frequency 1 Hz and voltage to distant ratio of 1300 V/cm [8, 12, 13]. For *in vivo* gene transfer pulse delivery protocols are still not standardized and the results of experimental studies are conflicting regarding the optimal pulse parameters for transfection [20-25]. Nevertheless, for efficient electrotransfection pulses should be much longer, even up to 20-50 ms pulses were suggested to be effective, but of lower amplitude (i.e. voltage to distance ratio 200 V/cm). Even better transfection efficiency can be obtained by combination of one short high-voltage permeabilization pulse followed by a number of long low-voltage electrophoretic pulses [27-28].

The application of large electric pulses to tissue causes not only electroporation, which is a non-thermal phenomenon, but may also cause concomitant heating. Namely, current flow through conducting medium involves Joule effect and consequently temperature increase in tissue can be expected. Temperatures above 43-45 °C cause denaturation of proteins and destruction of cell structures, eventually resulting in cell necrosis. Evidently, heating can become critical parameter especially for *in vivo* electrotransfection when reversible membrane permeabilization and cell survival is an imperative.

In our present study, we investigated possible effects of Joule heating during standard pulse delivery protocols used for electrochemotherapy and *in vivo* gene transfer, taking into account three dimensional geometry of tissue and electrodes, exact modeling of pulse trains, both the electrical and thermal properties of tissue and electrodes, contribution of blood perfusion and the

thermal contact with the surroundings. Based on the numerical simulations we analyze the influence of tissue electrical conductivity and parameters of electric pulses (amplitude, duration, number of pulses, pulse repetition frequency) on the temperature distribution within the tissue and the electrodes and compare our with previously published results [29-32].

2 METHODS

The significance of Joule heating as a mode of tissue damage during electroporation-based treatments can be estimated by determining the tissue temperature as a function of time. Because Joule heating involves electro-thermal interactions multiphysics modeling is required.

2.1 COUPLED ELECTRO-THERMAL MODEL

Electric field $\mathbf{E}$ induced in the tissue as a result of the voltage applied at the electrodes is usually modeled assuming the tissue to be a passive homogenous linear volume conductor [33, 29, 30]. Supposing that the electric current density $\mathbf{J}$ in tissue is divergence-free, the electric potential φ satisfies:

$$\nabla \cdot (\sigma \nabla \varphi) = 0 \qquad (1)$$

where σ is the electrical conductivity. Moreover, electric field can be further expressed as a gradient of scalar electric potential $\mathbf{E} = -\nabla \varphi$, and current density is related to electric field by Ohm's law $\mathbf{J} = \sigma \mathbf{E}$. In this formulation the displacement current $\mathbf{J}_{disp} = \varepsilon_r \varepsilon_0 (\partial \mathbf{E} / \partial t)$, with ε_r known as relative permittivity, and the magnetic induction effect have been neglected as non-dominant effects. Also, in spite of the fact that at electroporative field strength tissue conductivity increases [34-36] (i.e. tissue is not a linear conductor), we decided to use linear model and take this nonlinear effect into account by parametrization of tissue conductivity. Namely, recently presented macroscopic model of tissue electropermeablization that includes the increase of tissue conductivity with the electric field intensity [36], would be too difficult to couple with the equation describing the heat transfer.

Heat transfer in the tissue under normal conditions can be modeled by the bioheat equation proposed by Pennes [37]. However, exposure of tissue to electric pulses requires Joule heating to be taken into account. Thus, in our model, the temperature T is obtained from the bioheat equation in which the Joule heating term $\mathbf{JE}$ is added as a distributed heat source:

$$\rho c \frac{\partial T}{\partial t} = \nabla \cdot (k \nabla T) - \rho_b \omega_b c_b (T - T_b) + Q_m + \mathbf{JE} \quad (2)$$

Here t is the time, ρ, c and k are the density, the heat capacity and the thermal conductivity of tissue, ω_b is the blood perfusion, ρ_b and c_b are the density and the heat capacity of blood, T_b is the temperature of the arterial blood and Q_m is the metabolic heat. Due to time dependent diffusion process, thermal modeling is more complex than electrical.

Together with appropriate boundary and initial conditions, equations (1) and (2) represent complete formulation of the problem in the form of two partial differential equations. These two equations are coupled and have to be solved simultaneously. Namely, heating power per unit volume due to the Joule effect:

$$\mathbf{JE} = \sigma |\mathbf{E}|^2 = \sigma |\nabla \varphi|^2 \qquad (3)$$

which can be obtained from the solution of the first equation (1) acts as a distributed heat source in the heat equation (2). As tissue electrical conductivity increases with temperature [38], additional coupling between equations (1) and (2) exist. This temperature dependence of tissue electrical conductivity is modeled as:

$$\sigma = \sigma_0 \left[1 + \alpha \left(T - T_0 \right) \right] \qquad (4)$$

where α is the temperature coefficient. For most tissues it is around 1.5 % /ºC [38].

We applied the finite-element approach to solve the formulated coupled electro-thermal model for specific electrode configurations and different pulse protocols. We used COMSOL Multiphysics (COMSOL AB, Sweeden) environment with MATLAB (The MathWorks, Inc. USA) for geometry modeling, meshing and solving.

2.2 GEOMETRY MODELING AND MESHING

We developed geometrical models of two types of electrodes widely used for *in vivo* tissue electroporation: parallel plate electrodes (Figure 1) and a pair of needle electrodes (Figure 2).

In the case of plate electrodes, we modeled a block of tissue encompassed by two parallel stainless steel plate electrodes placed 4.4 mm apart, mimicking *in vivo* electroporation experiment on rat liver. The length (x), the width (y) and the thickness (z) of each electrode were 20 mm, 6 mm and 0.5 mm, respectively. Since two symmetry planes exist (xy and xz) only one forth of the model presented in Figure 1 was actually modeled and meshed. The mesh consisted of approximately 30000 linear tetrahedral elements.
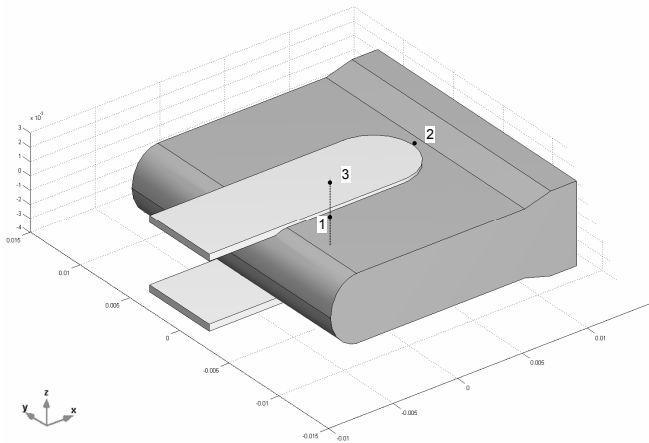
Figure 1. Geometrical model of plate electrodes and tissue. Electrode length (x) 21 mm, width (y) 6 mm, thickness (z) 0.5 mm; interelectrode distance: 4.4 mm. Numbers (1, 2 and 3) indicate selected locations for temperature comparison.
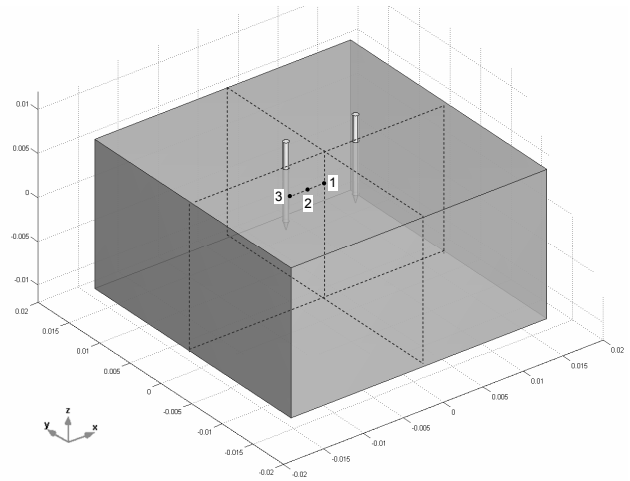
Figure 2. Geometrical model of needle electrodes and tissue. Needle diameter: 0.7 mm; insertion depth: 7 mm; interelectrode distance: 8 mm. Numbers (1, 2 and 3) indicate selected locations for temperature comparison.

In the case of needle electrodes, a block of tissue was modeled as a parallelepiped of 32 mm × 32 mm × 17 mm in which two needle electrodes 0.7 mm in diameter were inserted to the depth of 7 mm with interelectrode spacing 8 mm. The size of the tissue block, interelectrode distance, needle diameter and the insertion depth are the same as in the previous work [33]. Due to two symmetry planes, we meshed just one forth of the entire geometry, as for plate electrodes. Precaution was taken to obtain high quality mesh near the needles, where steep change of electric potential is expected. The final mesh of one quarter of the geometry shown in Figure 2 consisted of approximately 23000 linear tetrahedral elements.

2.3 TISSUE PROPERTIES AND BOUNDARY CONDITIONS

Since great number of electroporation studies was performed on rat liver, we assumed rat liver tissue for all our simulations. Physical properties of liver needed for our model described in section 2.1 can be found in literature [38, 39]. The most important parameter that determines electric conduction through tissue is electrical conductivity. Nominal low-frequency (at 10 Hz) electrical conductivity of rat liver that we used in this study was 0.126 S/m [38], which is very close to reports of liver conductivity by Duck (0.12 S/m) [39] and by Foster and Schwan (0.13 S/m) [40], and is slightly higher than conductivity measured by Gabriel et al. (0.07 S/m) [41]. This nominal conductivity means the conductivity of non-electroporated tissue. We already mentioned that tissue conductivity increases due to electroporation. To analyze how this increase affects the temperature rise in the tissue we performed simulations also for 2 and 4 times higher electrical conductivity from the nominal conductivity (i.e. 0.252 S/m and 0.504 S/m). This simplification introduces some error, since in real situation tissue conductivity increases nonuniformly depending on the local electric field intensity (i.e. only where electroporation occur). Also, the extent of assumed conductivity increase is on a high side. However, this parameterization analysis enables to simulate the worst-case scenario to predict the maximum temperature rise. Another useful

aspect of conductivity parametrization is the possibility of reinterpreting the simulation results for tumors since electrical conductivity of hepatic tumors (at 10 Hz) is 0.269 S/m [38], which is approximately two times higher than the conductivity of normal liver tissue. The values of liver tissue density (ρ =1050 kg/m^3), heat capacity (c=3600 J/(kg·K)), thermal conductivity (k=0.512 W/(m·K)), temperature coefficient of electrical conductivity (α =1.5% ºC^{-1}) are also taken from the literature [39]. Electrodes, made of stainless steel, were modeled with both electrical and thermal properties (electrical conductivity σ =1.398×10^6 S/m, density ρ =1050 kg/m^3, heat capacity c=490 J/(kg·K), thermal conductivity k=16.3 W/(m·K)). Blood density and heat capacity are ρ_b =1060 kg/m^3 and c_b = 3600 J/(kg·K) respectively [39]. Normal blood perfusion for liver was estimated to 0.0044 s^{-1} from literature data originally expressed in ml/(100 g·min) [42], and the metabolic heat was assumed to be Q_m =420 W/m^3 [43].

Driving of electrodes with pulse trains was modeled as time dependent Dirichlet boundary condition. Schematic representation of high-voltage (HV) and low-voltage (LV) pulse trains used in simulations is given in Figure 3. For electochemotherapy case, where short high-voltage pulses are used, we performed simulations for a train of 8 square-wave pulses of 100 μs duration. Pulse amplitude was chosen to obtain voltage-to-distance ratio of 1500 V/cm for both electrode geometries. Thus, the pulse amplitude was 660 V for plate electrodes and 1200 V for needle electrodes. The voltage-to-distance ratio (or the nominal applied electric field) differs from the actual electric field in tissue. In particular this is true for needle electrodes that have steep decrease of the field in the radial direction. However, we used voltage-to-distance ratio for convenience, to be inline with reported data from experimental studies. Pulse repetition frequency was 1 Hz (standard) and 1 kHz (high). We denote this high-voltage pulse train as HV: 1500 V/cm, 8×100 μs, 1 Hz (or 1 kHz). For electrotransfection case, we simulated a train of long low-voltage pulses delivered every 1 s each having the amplitude 110 V for plate electrodes and 200 V for needle electrode (corresponding to voltage-to-distance ratio 250 V/cm) and pulse duration of 50 ms (LV: 250 V/cm, 8×50 ms, 1 Hz). This protocol was chosen since it was the most effective for electrotransfection of rat liver [21]. Due to symmetry, boundary condition on electrode was half the actual voltage, and symmetry plane between electrodes was treated as antismmetry boundary condition (i.e. zero potential). Other boundaries were treated as electrically insulating.

Thermal boundary conditions were insulation on all boundaries except the upper surface of tissue and electrodes which was modeled as convective boundary condition. Initial tissue temperature was assumed to be 37ºC. Temperature of surrounding air was set to 25ºC, and convective heat-transfer coefficient is set to 10 W/(m^2 K).

For pulse trains having 1 Hz repetition frequency simulations were run for 10 s. Since the duty cycle is very low (i.e. for HV pulses 100 μs / 1 s = 10^{-4}) special attention was given to the control of time steps in the variable-step solver. For pulse trains having 1 kHz repetition frequency simulations were run for 8.5 ms. This is sufficient simulation time, since all pulses are delivered in 8 ms and the highest tissue temperature is expected

immediately after the end of the last pulse and the peak tissue temperature can thus be estimated.
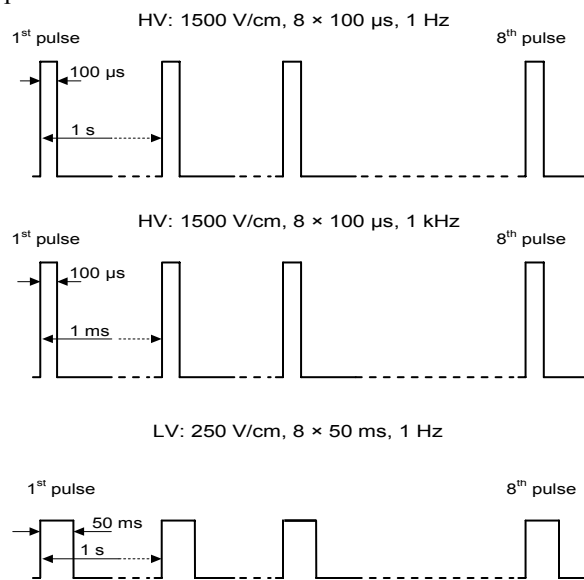


Figure 3. Schematic representation of high-voltage (HV) and low-voltage (LV) pulse trains used in simulations.

3 RESULTS

The computed temperature distribution for all cases studied would take too much space, so we present only some characteristic cases. The results are organized to compare different electrode geometries (plates, needles), different pulse protocols (electrochemotherapy, high frequency electrochemotherapy and electrotransfection), and all parametrized for different tissue electrical conductivities. In order to evaluate the time course of temperature during a train of voltage pulses we selected three characteristic locations in each geometrical model. For plate electrodes (Figure 1) these locations are: 1 - in the tissue exactly in the middle between the two electrodes; 2 - in the tissue near (0.1 mm) the tip of the electrode; and 3 - in the electrode itself. For needle electrodes (Figure 2) these locations lie in the *xy* plane at the depth of 3.5 mm from the tissue surface and their position are: 1 - in the tissue exactly in the middle between electrodes; 2 - in the tissue 2 mm radially from the electrode surface (in the direction of the opposite electrode); and 3 - in the tissue near (0.1 mm) the electrode.

First we consider standard electrochemotherapy protocol with plate electrodes. Temperature distribution immediately after the last pulse in the train of eight short HV pulses (1500 V/cm, 8×100 μs, 1 Hz) is presented in Figure 4. Note that only one forth of the entire model is shown. Due to the symmetry, solutions in other parts of the geometry are easily obtained by mirroring. However, we prefer this view since it exposes the interior of the tissue and electrodes. Simulation results for nominal (0.126 S/m) and increased (0.504 S/m) tissue electrical conductivity are given. Time course of temperature at selected locations is presented below the spatial distribution of the temperature (Figure 4c). Since temperature plots overlap, to avoid ambiguity, we point out that temperature at location 1 exhibits staircase-like increase, while at location 2 has spiky transients.

HV pulses: 1500 V/cm, 8×100 µs, 1 Hz

(a)

(b)

(c)
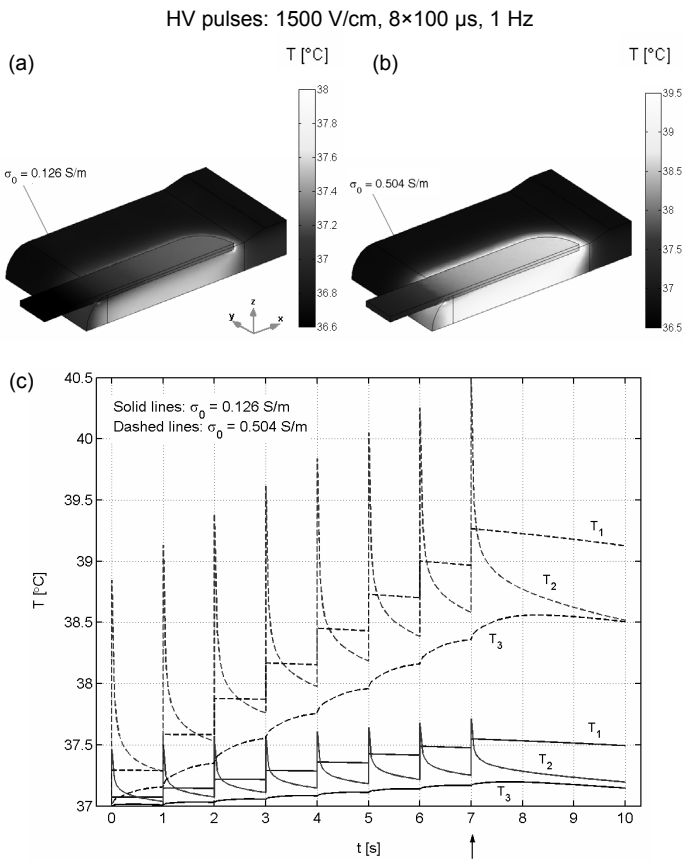
Figure 4. Temperature distribution for plate electrodes immediately after the last pulse in the train of eight short HV pulses (1500 V/cm, 8×100 µs, 1 Hz) for two values of tissue electrical conductivity: (a) 0.126 S/m (nominal) and (b) 0.504 S/m (increased). Note different temperature scales. (c) Time course of temperature in selected points. Marker (↑) indicates the time step corresponding to the temperature distributions shown in Figures 4a and 4b. Exact location of the selected points is shown in Figure 1.

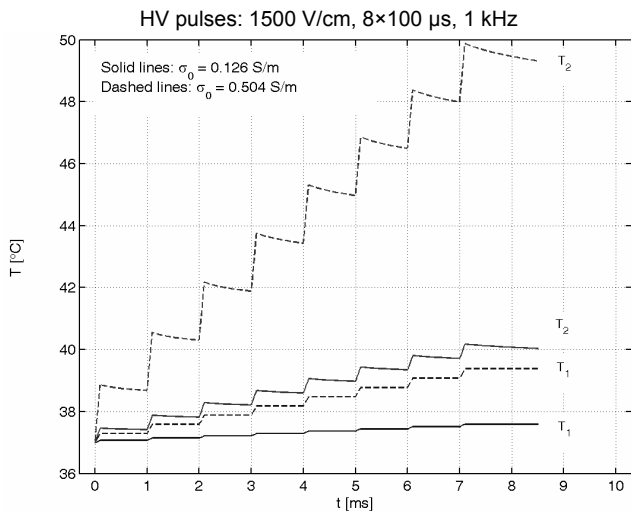LV pulses: 250 V/cm, 8×50 ms, 1 Hz

(a)

(b)

(c)
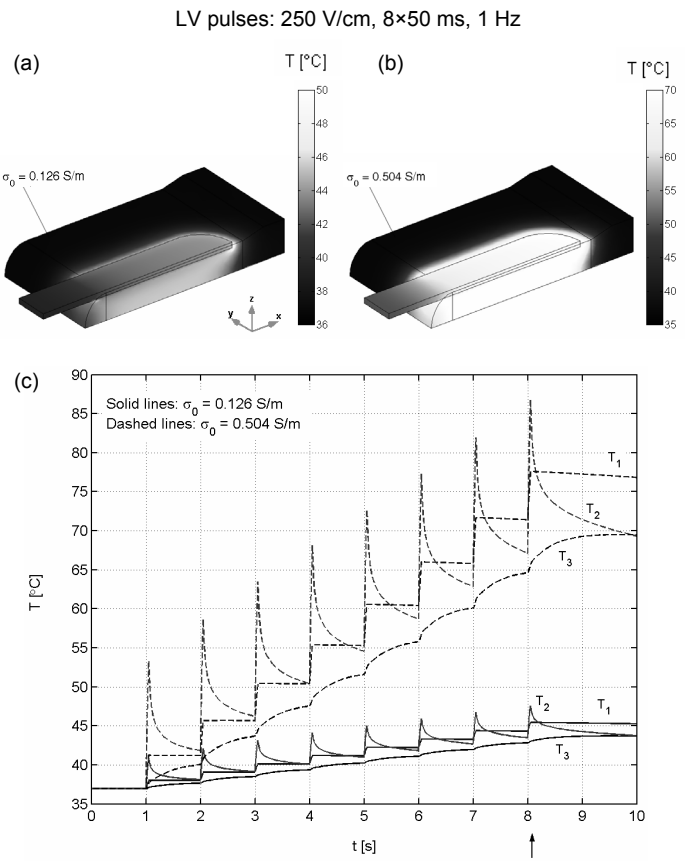
Figure 6. Temperature distribution for plate electrodes immediately after the last pulse in the train of eight long LV pulses (250 V/cm, 8×50 ms, 1 Hz) for two values of tissue electrical conductivity (a) 0.126 S/m (nominal) and (b) 0.504 S/m (increased). Note different temperature scales. (c) Time course of temperature in selected points. Marker (↑) indicates the time step corresponding to the temperature distributions shown in Figures 4a and 4b. Exact location of the selected points is shown in Figure 1.

The influence of increased pulse repetition frequency on temperature rise for plate electrodes is given in Figure 5. For clarity, we only report tissue temperature at locations 1 and 2 for two different tissue conductivity values.

Figure 6 illustrates the temperature distribution and time course of temperature at selected locations for the train of eight long LV pulses (250 V/cm, 8×50 ms, 1 Hz) again for plate electrodes with tissue electrical conductivity as a parameter. These simulation results illustrate Joule heating during electrotransfection with plate electrodes.

LV pulses were delivered intentionally with 1 s delay to check the contribution of air convection. It was found that after 1 s the temperature drop due to air convection is less than 0.05ºC even at the tissue surface (location 3).

The three figures to follow (Figures 7, 8 and 9) show, for needle electrodes, the same as previous three figures for plate electrodes i.e. calculated temperature distributions for standard electrochemotherapy protocol, for high frequency electrochemotherapy and for electrotransfection protocol. Thus, Figure 7 presents the response of needle electrode model to HV pulses (1500 V/cm, 8×100 µs, 1 Hz), Figure 8 shows the same for 1 kHz HV pulses (1500 V/cm, 8×100 µs, 1 Hz) and Figure 9 illustrates results for LV pulses (250 V/cm, 8×50 ms, 1 Hz).

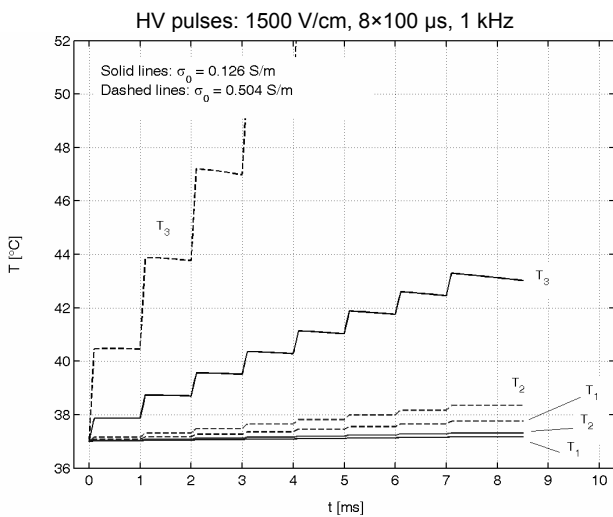HV pulses: 1500 V/cm, 8×100 µs, 1 kHz

Figure 5. Time course of temperature in selected points for plate electrodes during the train of eight short HV pulses (1500 V/cm, 8×100 µs, 1 kHz) for two values of tissue electrical conductivity 0.126 S/m (nominal) and 0.504 S/m (increased).
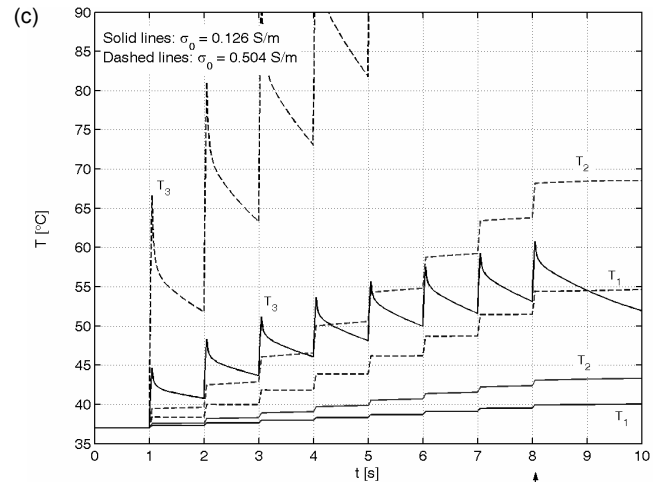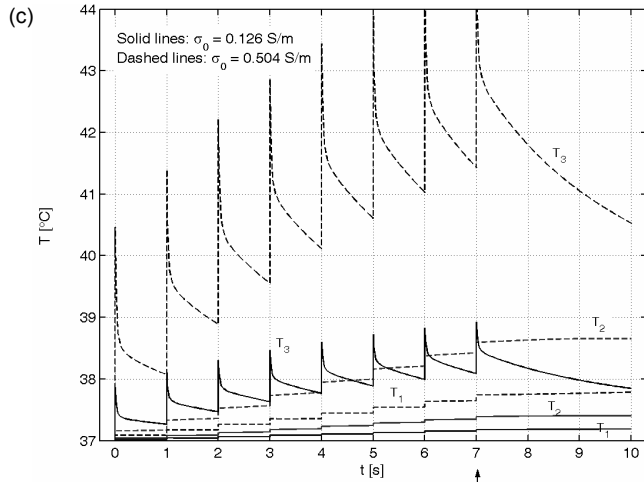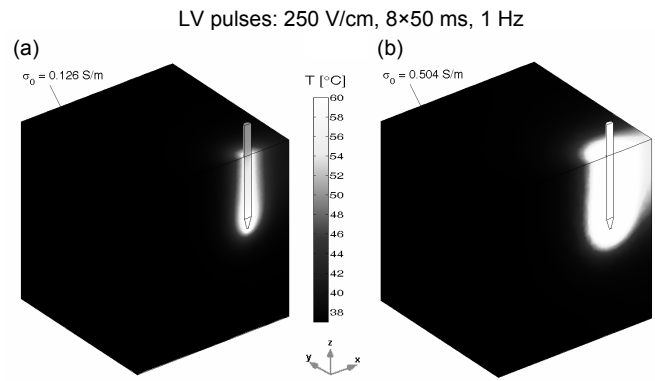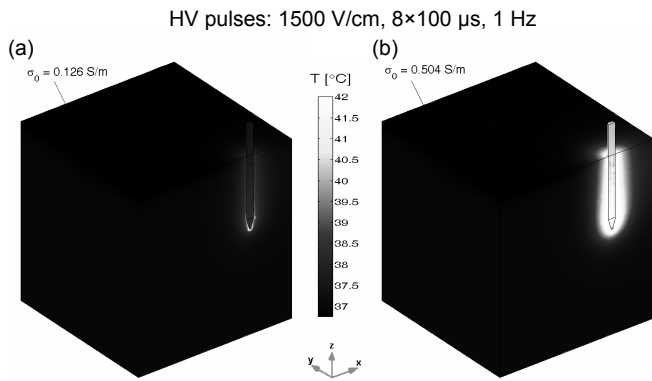
Figure 7. Temperature distribution for needle electrodes immediately after the last pulse in the train of eight short HV pulses (1500 V/cm, 8×100 μs, 1 Hz) for two values of tissue electrical conductivity: (a) 0.126 S/m (nominal) and (b) 0.504 S/m (increased). Note different temperature scales. (c) Time course of temperature in selected points. Marker (↑) indicates the time step corresponding to the temperature distributions shown in Figures 7a and 7b. Exact location of the selected points is shown in Figure 2. The temperature at location 3 for 0.504 S/m (T_3, dashed line) peaks at 45°C.

Figure 9. Temperature distribution for needle electrodes immediately after the last pulse in the train of eight long LV pulses (250 V/cm, 8×50 ms, 1 Hz) for two values of tissue electrical conductivity (a) 0.126 S/m (nominal) and (b) 0.504 S/m (increased). Note different temperature scales. (c) Time course of temperature in selected points. Marker (↑) indicates the time step corresponding to the temperature distributions shown in Figures 4a and 4b. Exact location of the selected points is shown in Figure 1. The temperature at location 3 for 0.504 S/m (T_3, dashed line) peaks at 139°C.

To avoid ambiguity in interpretation, we point out that in Figures 7c and 9c, temperature at locations 1 and 2 exhibits staircase-like increase, while at location 3 has spiky transients.

4 DISCUSSION

Application of large electric fields to cells results in the build-up of a transmembrane voltage. At sufficiently large external field strength, the intense electric field that develops across the cellular membrane causes structural rearrangements in the membrane and formation of pores. This process of electroporation is reversible at formative field strengths and becomes irreversible at higher levels. It is a multistage process with a very rapid onset of the formation of conduction pathways in the membrane. Along with pure electric field effect, thermal reactions from the passage of electric current occur. There have been several studies investigating Joule heating during skin electroporation, where localized heating in the stratum corneum was analyzed and theoretical model of temperature rise was developed [44-46]. These studies were aimed primarily to study

Figure 8. Time course of temperature in selected points for needle electrodes during the train of eight short HV pulses (1500 V/cm, 8×100 μs, 1 kHz) for two values of tissue electrical conductivity 0.126 S/m (nominal) and 0.504 S/m (increased). The temperature at location 3 for 0.504 S/m (T_3, dashed line) peaks at 62°C.

the thermal effects of electroporation on a microscale. Temperature rise due to Joule heating during solid tissue electroporation was studied experimentally on animal tissue *ex vivo* and by two-dimensional finite-element model [29]. Theoretical analysis of thermal effects during *in vivo* tissue electroporation was published, but was also limited to two dimensions, with additional simplifications regarding modeling of pulse trains [30]. During the last few years, irreversible electroporation emerged as an independent non-thermal modality for tissue ablation including tumors [47-50]. Temperature considerations during irreversible electroporation were studied on multicellular model and on a multiscale tissue model constructed from a unit cell [31]. Recently, a study investigating temperature effects associated with irreversible electroporation based on a bulk tissue model was published [32]. This study is also two-dimensional, pulse trains are not modeled and results are due to normalization in time and temperature hard to directly apply to specific pulsing protocol. Our present study contributes, at the macroscopic level, to more realistic modeling of tissue heating for electrochemotherapy and *in vivo* gene electrotransfer.

Theoretically, under the assumption of adiabatic conditions and homogenous electric field between the electrodes, the law of the conservation of energy, gives the following temperature increase after a single electric pulse of the duration t_p and amplitude V_0 :

$$\Delta T_1 = \frac{\sigma_0 V_0^2 t_p}{\rho c d^2} \tag{5}$$

where d is the distance between the electrodes, σ_0 , ρ and c are tissue electrical conductivity, mass density and heat capacity, respectively. After N pulses, cumulative temperature rise can be estimated as $\Delta T_N = N \Delta T_1$. However, with realistic plate and needle electrodes, the application of equation (5) for estimating the increase of tissue temperature related to pulse trains used in electrochemotherapy and electotransfection would give erroneous results. One aspect is complex geometry where even for plate electrodes actual electric field differs from imposed voltage-to-distance ratio. Another aspect is that equation (5) gives the upper limit of the temperature rise in the bulk of the tissue, since numerous factors contributing to heat sinking are not taken into account. Specifically, equation (5) neglects the presence of electrodes, their finite dimensions and material properties, heat diffusion in the tissue and electrodes, thermal contact with the surroundings and the contribution of blood perfusion. Moreover, equation (5) neglects the edge effects where heating is much higher than in the bulk and also the increase of electrical conductivity of tissue due to the temperature rise. To take all these effects into account we formulated the problem with partial differential equations (1) and (2), and decided to do three-dimensional geometry modeling. The effect of the increase of tissue electrical conductivity caused by electroporation we addressed by parametrization. We focused on three-dimensional finite element modeling of electric and thermal fields in liver tissue exposed to high- and low-voltage pulse trains that were delivered through the parallel plate or needle electrodes. We obtained the electric field and temperature distribution in the tissue for the typical pulse train for electrochemotherapy (1500 V/cm, 8×100 μs, 1 Hz), for electrochemotherapy with high repetition frequency pulses (1500 V/cm, 8×100 μs, 1 Hz) and for a widely used pulse train for *in vivo* electrotransfection (250 V/cm, 8×50 ms, 1 Hz).

Before commenting on the results of our simulations, the temperature threshold for thermal damage is important aspect to consider. Thermal damage depends on the duration of exposure and the temperature. Survey of high-voltage and high-current injuries by M. A. Chilbert provides information for some tissues [51]. Cutaneous burns occur when the temperature is elevated for a sufficient length of time: 45ºC requires more than 3 h, 51ºC requires less than 4 min and 70ºC requires less than 1 s. Temperature levels that cause injury in other tissues are similar, although for example, electrically induced thermal damage to peripheral nerve has been noted to occur at 48ºC after several seconds. For the interpretation of our results we assume that for temperatures less than 43ºC no cellular injury occurs. Temperatures above 43-45°C cause denaturation of proteins and destruction of cell structures, eventually resulting in cell necrosis. If the tissue temperature is transiently increased but kept below 45-50°C thermal damage is likely to be insignificant. Higher temperatures can lead to tissue thermal damage, with undesirable consequences on the success of electrochemotherapy or electrotransfection.

We see from the results (Figure 4 – Figure 9) that tissue temperature due to Joule heating strongly depends on electrode geometry, tissue electrical conductivity, and on parameters of electric pulses - pulse duration, pulse amplitude, repetition frequency and the number of pulses.

For standard electrochemotherapy protocol (HV pulses: 1500 V/cm, 8×100 μs, 1 Hz) with plate or needle electrodes tissue heating is observed but is not critical (Figure 4 and Figure 6) even if we assume considerably (4×) increased tissue conductivity. The results also show that successive HV pulses cumulatively increase the bulk tissue temperature. Namely, there is no cooling of the bulk tissue between the pulses although pulses are much shorter than the pauses between them (100 μs vs. 1 s). Cooling between pulses is observed only in the vicinity of electrodes due to strong temperature gradient between the tissue and electrode (Figure 4c trace T_2 , and Figure 7c, trace T_3). Temperature of electrodes also increases (i.e Figure 4c trace T_3) due to heat conduction from the tissue (as opposed to modeling of electrodes in [29] as infinite heat sinks at 37ºC). Indeed, electrodes serve as heat sinks, but due to relatively small volume their temperature quickly rises. For needle electrodes, the results show highly localized tissue heating with maximal temperature rise in the bulk near the electrode tip. The region of increased temperature is formed around the needles where electric field and current density are the highest. This region overlaps with regions where electroporation occurs [33, 36]. Due to spatial distribution of the electric field around needle electrodes, this part of tissue close to needles is most likely also irreversible electroporated. Simulation results are in agreement with experiments and prove the safety of standard electrochemotherapy pulsing protocol (up to 1500 V/cm, 8×100 μs, 1 Hz) with respect to tissue thermal damage.

With adequate local anesthesia, the main side-effect of electrochemotherapy is an unpleasant contraction of muscles located in the vicinity of the electrodes. Since the pulse repetition frequency of 1 Hz is most often used, each pulse in the train of 8 pulses causes the contraction of muscles innervated by the excited nerves. Electrochemotherapy with pulse repetition frequency above the frequency of tetanic contraction would reduce the number of individual muscle contractions and would improve patient comfort. Recent experimental studies where electrochemotherapy with high frequency pulses (e.g. 1 kHz [52] and 5 kHz [12, 53]) was performed have shown that using higher repetition frequency reduces the unpleasant contractions to a single one and shortens the treatment time, while the efficacy of electrochemotherapy measured by the tumor response to treatment was not different comparing to the standard 1 Hz protocol. Results of our simulations for high repetition frequency electrochemotherapy (HV pulses: 1500 V/cm, 8×100 μs, 1 kHz) for two electrode geometries (plate electrodes - Figure 5; needle electrodes – Figure 8) show that the increase of pulse repetition frequency from 1 Hz to 1 kHz causes an increase of bulk tissue temperature that is still low and unlikely to induce thermal damage (note that time scale is in ms). This result was validated in the most recent electrochemotherapy study on patients where, for the first time, pulse repetition frequency of 5 kHz was used and has proven to be safe and even more effective in tumor treatment than standard repetition frequency of 1 Hz [12]. However, from our simulation results we observe that near the electrodes temperature rise may be significant (Figure 5 trace T_2, Figure 8 trace T_3) if increased conductivity is assumed.

Simulation results for electrotransfection protocol with train of LV pulses (250 V/cm, 8×50 ms, 1 Hz) for both plate (Figure 6) and needle electrode (Figure 9) show that temperature increase in the tissue is far from being unimportant. The simulated train of electrophoretic pulses is likely to cause localized thermal damage, especially if we assume highly conductive tissue. This numerical result can explain tissue damage observed in some *in vivo* electrotransfection studies. For the success of electrotransfection, and minimization of thermal damage, careful optimization of pulsing protocol is necessary. This is particularly important if needle electrodes will be used. Therefore, to be within the 'safe range' either the pulse amplitude, duration or number should be reduced.

When comparing a pair of needles to parallel plate electrodes, with needles it is harder to avoid local tissue heating and to achieve, in a larger tissue volume, local electric field between reversible and irreversible permeabilization threshold. This is an important guideline for clinicians when considering appropriate electrode type for cancer electrochemotherapy or gene electro transfer.

5 CONCLUSIONS

Model-based analysis of Joule heating in electroporation-based treatments enables to predict temperature rise in tissue and electrodes during and after pulse delivery. This analysis provides useful insight into the extent of tissue thermal damage (if any) and provides important guidelines for development of electrodes and safe protocols for electrochemotherapy and gene electro therapy. Our results show that at specific pulse parameters at least locally tissue heating might be significant (i.e. tissue temperatures to grow in excess of 43ºC). For electrochemotherapy, this is not critical since regions of increased temperature are most likely irreversibly electroporated. However, DNA electrotransfer may be unsuccessful due to heating-related DNA damage.

ACKNOWLEDGMENT

This work was funded within the program of bilateral scientific cooperation between the Republic of Croatia and the Republic of Slovenia, and by national research grants from Slovenian Research Agency and from the Ministry of Science, Education and Sports of the Republic of Croatia.

REFERENCES

[1] M. Okino and H. Mohri, "Effects of a high-voltage electrical impulse and an anticancer drug on in vivo growing tumors", Jpn. J. Cancer Res., Vol. 78, pp. 1319-1321, 1987.
[2] L. M. Mir, S. Orlowski, J. Belehradek, and C. Paoletti, "Electrochemotherapy potentiation of antitumor effect of blemycin by local electric pulses", Eur. J. Cancer, Vol. 27, pp. 68-72, 1991.
[3] G. Sersa, M. Cemazar, D. Miklavcic, L. M. Mir, "Electrochemotherapy: variable anti-tumor effect on different tumor models", Bioelectrochem. Bioenerg., Vol. 35, pp. 23-27, 1994.
[4] G. Serša, M. Čemažar, and D. Miklavčič, "Antitumor effectiveness of electrochemotherapy with cis-diamminedichloroplatinum(II) in mice", Cancer Res., Vol. 55, pp. 3450-3455, 1995.
[5] R. Heller, M. Jaroszeski, J. Leo-Messina, R. Perrott, N. Van Voorhis, D. Reintgen, and R. Gilbert, "Treatment of B16 melanoma with the combination of electroporation and chemotherapy", Bioelectrochem. Bioenerg., Vol. 36, pp. 83-87, 1995.
[6] R. Heller, M. Jaroszeski, R. Perrott, J. Messina and R. Gilbert, "Effective treatment of B16 melanoma by direct delivery of bleomycin using electrochemotherapy", Melanoma Res., Vol. 7, pp. 10-18, 1997.
[7] R. Heller, M. J. Jaroszeski, D. S. Reintgen, C. A. Puleo, R. C. DeConti, R. A. Gilbert, and L. F. Glass, "Treatment of cutaneous and subcutaneous tumors with electrochemotherapy using intralesional bleomycin", Cancer, Vol. 83, pp. 148-157, 1998.
[8] L. M. Mir, L. F. Glass, G. Serša, J. Teissié, C. Domenge, D. Miklavčič, M. J. Jaroszeski, S. Orlowski, D. S. Reintgen, Z. Rudolf, M. Belehradek, R. Gilbert, M. P. Rols, J. Belehradek, Jr., J. M. Bachaud, R. DeConti, B. Štabuc, M. Čemažar, P. Coninx and R. Heller, "Effective treatment of cutaneous and subcutaneous malignant tumors by electrochemotherapy", Br. J. Cancer., Vol. 77, pp. 2336–2342, 1998.
[9] R. Heller, R. Gilbert and M. J. Jaroszeski, "Clinical applications of electrochemotherapy" Adv. Drug Deliv. Rev., Vol. 35, pp. 119-129, 1999.
[10] A. Gothelf A, Mir LM, and J. Gehl, "Electrochemotherapy: results of cancer treatment using enhanced delivery of bleomycin by electroporation", Cancer Treat. Rev., Vol. 5, pp. 371-387, 2003.
[11] G. Serša, M. Čemažar, and Z. Rudolf, "Electrochemotherapy: advantages and drawbacks in the treatment of patients", Cancer Therapy, Vol. 1, pp. 133-142, 2003.
[12] M. Marty, G. Sersa, J. R. Garbay, J. Gehl, C. G. Collins, M. Snoj, V. Billard, P. F. Geertsen, J. O. Larkin, D. Miklavcic, I. Pavlovic, S. M. Paulin-Kosir, M. Cemazar, N. Morsli, D. M. Soden, Z. Rudolf, C. Robert, G. C. O'Sullivan and L. M. Mir, "Electrochemotherapy - An easy, highly effective and safe treatment of cutaneous and subcutaneous metastases: Results of ESOPE (European Standard Operating Procedures of Electrochemotherapy) study", Eur. J. Cancer Suppl. Vol. 4, pp. 3-13, 2006.
[13] G. Serša, "The state-of-the-art of electrochemotherapy before ESOPE study: advantages and clinical uses", Eur. J. Cancer Suppl., Vol 4, pp. 52-59, 2006.

[14] G. Sersa, D. Miklavcic, M. Cemazar, Z. Rudolf, G. Pucihar and M. Snoj "Electrochemotherapy in treatment of tumours", Eur. J. Surg. Oncol. Vol. 34, pp. 232-240, 2008.

[15] T. Y. Tsong, "Electroporation of cell membranes", Biophys. J., Vol. 60, pp. 297-306, 1991.

[16] J. C. Weaver, and Y. A. Chizmadzhev, "Theory of electroporation: a review", Bioelectrochem. Bioenerg. Vol. 41, pp. 135-160, 1996.

[17] E. Neumann, S. Kakorin and K. Toensing, "Fundamentals of electroporative delivery of drugs and genes", Bioelectrochem. Bioenerg. Vol. 48, pp. 3-16, 1999.

[18] J. Teissié, N. Eynard, B. Gabriel, and M. P. Rols, "Electropermeabilization of cell membranes", Adv. Drug Deliv. Rev., Vol. 35, pp. 3-19, 1999.

[19] J. Teissié, M. Golzio, and M. P. Rols, "Mechanisms of cell membrane electropermeabilization: A minireview of our present (lack of?) knowledge", Biochim. Biophys. Acta - General Subjects, Vol. 1724, pp. 270-280, 2005.

[20] R. Heller, M. J. Jaroszeski, A. Atkin, D. Moradpour, R. Gilbert, J. Wands and C. Nicolau, "In vivo gene electroinjection and expression in rat liver", FEBS Letters, Vol. 389, pp. 225-228, 1996.

[21] T. Suzuki, B. C. Shin, K. Fujikura, T. Matsuzaki, and K. Takata, "Direct gene transfer into rat liver cells by in vivo electroporation". FEBS Letters, Vol. 425, pp. 436-440, 1998.

[22] L. M. Mir, M. F. Bureau, J. Gehl, R. Rangara, D. Rouy, J. M. Caillaud, P. Delaere, D. Branellec, B. Schwartz and D. Scherman, "High-efficiency gene transfer into skeletal muscle mediated by electric pulses", Proc. Natl. Acad. Sci. USA., Vol. 96 pp. 4262-4267, 1999.

[23] M. Bettan, M. A. Ivanov, L. M. Mir, F. Boissiere, P. Delaere, and D. Scherman, "Efficient DNA electrotransfer into tumors", Bioelectrochem., Vol. 52, pp. 83-90, 2000.

[24] M. F. Bureau, J. Gehl, V. Deleuze, L. M. Mir, and D. Scherman, "Importance of association between permeabilization and electrophoretic forces for intramuscular DNA electrotransfer", Biochim. Biophys. Acta, Vol. 1474, pp. 353-359, 2000.

[25] M. Čemažar, G. Serša, J. Wilson, G. M. Tozer, S. L. Hart, A. Grosel, and G. U. Dachs, "Effective gene transfer to solid tumors using different nonviral gene delivery techniques: Electroporation, liposomes, and integrin-targeted vector", Cancer Gene Ther., Vol. 9, pp. 399-406, 2002.

[26] M. Cemazar, M. Golzio, G. Sersa, M. P. Rols, and J. Teissié, "Electrically-assisted nucleic acids delivery to tissues in vivo: where do we stand?" Curr. Pharm. Des., Vol. 12, pp. 3817-3825, 2006.

[27] S. Šatkauskas, M. F. Bureau, M. Puc, A. Mahfoudi, D. Scherman, D. Miklavčič and L. M. Mir, "Mechanisms of in vivo DNA electrotransfer: respective contributions of cell electropermeabilization and DNA electrophoresis", Mol. Ther. Vol. 5, pp. 133-140, 2002.

[28] M. Kanduser, D. Miklavcic and M. Pavlin, "Mechanisms involved in gene electrotransfer using high- and low-voltage pulses — An in vitro study", Bioelectrochem. Vol. 74, pp. 265-271, 2009.

[29] U. Pliquett, "Joule heating during solid tissue electroporation", Med. Biol. Eng. Comput., Vol. 41, pp. 215–219, 2003.

[30] R. V. Davalos, B. Rubinsky, and L. M. Mir, "Theoretical analysis of the thermal effects during in vivo tissue electroporation", Bioelectrochem Vol. 61, pp. 99–107, 2003.

[31] A. T. Esser, K. C. Smith, T. R. Gowrishankar and J. C. Weaver, "Towards solid tumor treatment by irreversible electroporation: intrinsic redistribution of fields and currents in tissue", Technol. Cancer Res. Treat., Vol. 6, pp. 261-274, 2007.

[32] R. V. Davalos and B. Rubinsky, "Temperature considerations during irreversible electroporation", Int. J. Heat and Mass Transfer, Vol. 51, pp. 5617-5622, 2008.

[33] D. Miklavcic, D. Semrov, H. Mekid, and L. M. Mir, "A validated model of in vivo electric field distribution in tissues for electrochemotherapy and for DNA electrotransfer for gene therapy", Biochim. Biophys. Acta Vol. 1523, pp. 233–239, 2000.

[34] M. Hibino, M. Shigemori, H. Itoh, K. Nagayama and K. Kinosita, "Membrane conductance of an electroporated cell analyzed by submicrosecond imaging of transmembrane potential", Biophys. J., Vol. 59, pp. 209–220, 1991.

[35] M. Pavlin, M. Kandušer, M. Rebersek, G. Pucihar, F. X. Hart, R. Magjarevic and D. Miklavcic, "Effect of cell electroporation on the conductivity of a cell suspension", Biophys. J., Vol. 88, pp. 4378–4390, 2005.

[36] D. Sel, D. Cukjati, D. Batiuskaite, T. Slivnik, L. M. Mir, and D. Miklavcic, "Sequential finite element model of tissue electropermeabilization", IEEE Trans. Biomed. Eng., Vol. 52, pp. 816–827, 2005.

[37] H. H. Pennes, "Analysis of tissue and arterial blood temperatures in the resting human forearm", J. Appl. Physiol., Vol. 85, pp. 5–34, 1998 (reprint; originally published in 1948).

[38] D. Haemmerich, S. T. Staelin, J. Z. Stai, S. Tungjitkusolmun, D. M. Mahvi, and J. G. Webster, "In vivo electrical conductivity of hepatic tumours", Physiol. Meas. Vol. 24, pp. 251–260, 2003.

[39] F. A. Duck, *Physical properties of tissue: A comprehensive reference book*, Academic Press, London, 1990.

[40] K. R. Foster and H. P. Schwan. "Dielectric properties of tissues and biological materials: A critical review", Crit. Rev. Biomed. Eng., Vol 17, pp. 25–104, 1989.

[41] S. Gabriel, R. W. Lau and C. Gabriel, "The dielectric properties of biological tissues: II. Measurement in the frequency range 10 Hz to 20 GHz", Phys. Med. Biol., Vol. 41, pp. 2251–2269, 1996.

[42] J. A. Davidson, S. Gir and J. Paul "Heat transfer analysis of frictional heat dissipation during articulation of femoral implants", J. Biomed. Mat. Res., Vol. 22, pp. 281–309, 1988.

[43] Y.-G. Lv, and J. Liu "A theoretical way of distinguishing the thermal and non-thermal effects in biological tissues subjected to EM radiation", Forschung im Ingeniuerwesen. Vol. 67, pp.242–253, 2003.

[44] G. T. Martin, U. F. Pliquett, J. C. Weaver, "Theoretical analysis of localized heating in human skin subjected to high voltage pulses", Bioelectrochem., Vol. 57, pp. 55-64, 2002.

[45] U. F. Pliquett, G. T. Martin and J. C. Weaver, "Kinetics of the temperature rise within human stratum corneum during electroporation and pulsed high-voltage iontophoresis", Bioelectrochem., Vol. 57, pp. 65-72, 2002.

[46] U. Pliquett, S. Gallo, S. W. Hui, Ch. Gusbeth and E. Neumann, "Local and transient structural changes in stratum corneum at high electric fields: contribution of Joule heating", Bioelectrochem., Vol. 67, pp. 37-46, 2005.

[47] B. Rubinsky, "Irreversible Electroporation in Medicine", Technol. Cancer Res. Treatment, Vol. 6, pp. 255-260, 2007.

[48] R. Davalos, L. M. Mir and B. Rubinsky "Tissue ablation with irreversible electroporation", Annals Biomed. Eng., Vol. 33, pp. 223-231, 2005.

[49] J. F. Edd, L. Horowitz, R. V. Davalos, L. M Mir, and B. Rubinsky, "In vivo results of a new focal tissue ablation technique: irreversible electroporation", IEEE Trans. Biomed. Eng., Vol. 53, pp. 1409-1415, 2006.

[50] B. Al-Sakere, F. André, C. Bernat, E. Connault, P. Opolon, R. V. Davalos, B. Rubinsky and L. M. Mir, "Tumor Ablation with Irreversible Electroporation", PLoS ONE, Vol. 2, e1135, 2007.

[51] J.P. Reilly "Electrical stimulation and electropatology", Cambridge University Press, pp. 383-428, 1992.

[52] I. Daskalov, N. Mudrov, and E. Peycheva, "Exploring new instrumentation parameters for electrochemotherapy. Attacking tumors with bursts of biphasic pulses instead of single pulses", IEEE Eng. Med. Biol. Mag., Vol. 18, pp. 62-66, 1999.

[53] A. Zupanic, S. Ribaric, and D. Miklavcic, "Increasing the repetition frequency of electric pulse delivery reduces unpleasant sensations that occur in electrochemotherapy", Neoplasma, Vol. 54, pp. 246-250, 2007.

Igor Lacković (M'03) was born in Karlovac, Croatia, in 1972. He received the B.Sc., M.Sc. and Ph.D. degrees in electrical engineering from the University of Zagreb, Zagreb, Croatia. He is currently an Assistant Professor with the Faculty of Electrical Engineering and Computing, University of Zagreb. His main research interests are in the field of biomedical engineering with a special focus on electric field interaction with biological tissue including numerical modeling of electric and thermal field distribution for electroporation-based drug and gene delivery, bioimpedance and related instrumentation development.

Ratko Magjarević (M'96) was born in Zagreb, Croatia in 1959. He received the Ph.D. degree in electrical engineering from the University of Zagreb, Zagreb. He is currently a Professor with the Faculty of Electrical Engineering and Computing, University of Zagreb. His main research interest is in biomedical engineering, in particular in the research of the influence of electric current and fields on tissue, cardiac pacing and bioimpedance measurements. He is Secretary General of the IFMBE.

Damijan Miklavčič was born in Ljubljana, Slovenia, in 1963. He received the Ph.D. degree in electrical engineering from the University of Ljubljana, Ljubljana. He is currently a Professor with the Faculty of Electrical Engineering and the Head of the Laboratory of Biocybernetics, University of Ljubljana. He is active in the field of biomedical engineering. His recent research interest focuses on electroporation-assisted drug and gene delivery, including cancer treatment by means of electrochemotherapy, tissue oxygenation, and modeling.